LIMNOLOGY and OCEANOGRAPHY

ASLO

*Limnol. Oceanogr.* 64, 2019, 93–108

doi: 10.1002/lno.11021

# Optically based quantification of fluxes of mercury, methyl mercury, and polychlorinated biphenyls (PCBs) at Berry's Creek tidal estuary, New Jersey

**G. Chang,[1]* T. Martin,[2] K. Whitehead,[3] C. Jones,[1] F. Spada[1]**

[1]Integral Consulting Inc., Santa Cruz, California
[2]Integral Consulting Inc., Salt Lake City, Utah
[3]Integral Consulting Inc., Olympia, Washington

## *Abstract*

Berry's Creek is an urban tidal estuary of the Hackensack River (New Jersey, U.S.A.), with over 10 km of waterways and over 3 km$^2$ of tidal marsh. More than a century of industrial activity has resulted in elevated contaminant concentrations in sediment, water, and biota. Mercury, methyl mercury, and polychlorinated biphenyls (PCBs) have been identified as the primary chemicals of concern (COCs) due to their persistence and bioaccumulation potential in aquatic and nearshore wildlife. As part of a multi-phased remedial investigation program, OPTically-based In-situ Characterization System (OPTICS) field studies were conducted in Berry's Creek to characterize water column contaminant dynamics, specifically to (1) improve understanding of the interrelationship(s) between surface sediment and water column contaminants and (2) quantify the transport of water column COCs between waterways and marshes. Results from OPTICS monitoring indicated that particulate resuspension from the upper 5 mm of the sediment bed during flood and ebb tides and storm flows is the primary process by which COCs are exchanged from bedded sediment to the water column. Analysis of mass exchange of COCs indicated that COCs associated with resuspended particulates are transported from the waterways to the marshes, where they are retained. Dissolved COC exchange from marshes to the waterways was minor (less than 8% of total COC mass in water). Overall, marshes were observed to be net sinks for COCs.

The Berry's Creek watershed, located in the Meadowlands of northern New Jersey (U.S.A.) (Fig. 1), has been affected by industrial activities since as early as the late nineteenth century. These activities have resulted in elevated concentrations of various chemical contaminants in the sediment, water column, and biota. Three industrial sites adjacent to Berry's Creek were added to the National Priorities List as Superfund sites in 1983 and 1984. The United States Environmental Protection Agency (USEPA) defined the entire Berry's Creek watershed as the Berry's Creek Study Area (BCSA) under the Comprehensive Environmental Response, Compensation, and Liability Act (CERCLA) and a detailed characterization of the tidal portion of the watershed was completed between 2008 and 2015 to support decision-making regarding potential remedial actions. Site characterization studies identified mercury, methyl mercury, and polychlorinated biphenyls (PCBs) as the primary chemicals of concern (referred to collectively herein as COCs) within the estuary. The potential ecological and human health risks associated with these COCs in this region as well as other locations has been well-documented (e.g., Letz 1983; Mergler et al. 2007 and references therein; Scheuhammer et al. 2007 and references therein; Weis and Ashley 2007; Chen et al. 2009, 2014).

The COCs within the sediment and water column (also referred to as surface water) in the BCSA estuary (including the main channel waterways, marsh tributary waterways, and the marshes) have the potential to accumulate in fish and other aquatic life to levels that might pose a risk to human health or ecological receptors. While the majority of COCs are found buried in sediment below the surface layer, COC concentrations in the surface sediments remain above regional background levels in the upstream portions of the site, which contributes significantly to biological exposure of estuarine organisms (Wright and Blauvelt 2010; Chen et al. 2014; BCSA Group 2018). Further, there are multiple mechanisms that redistribute COCs, including marsh-waterway exchange and resuspension of particle-bound chemical contaminants from the sediment bed to the water column. Therefore, an understanding of COC transport and exchange mechanisms across

*Correspondence: gchang@integral-corp.com

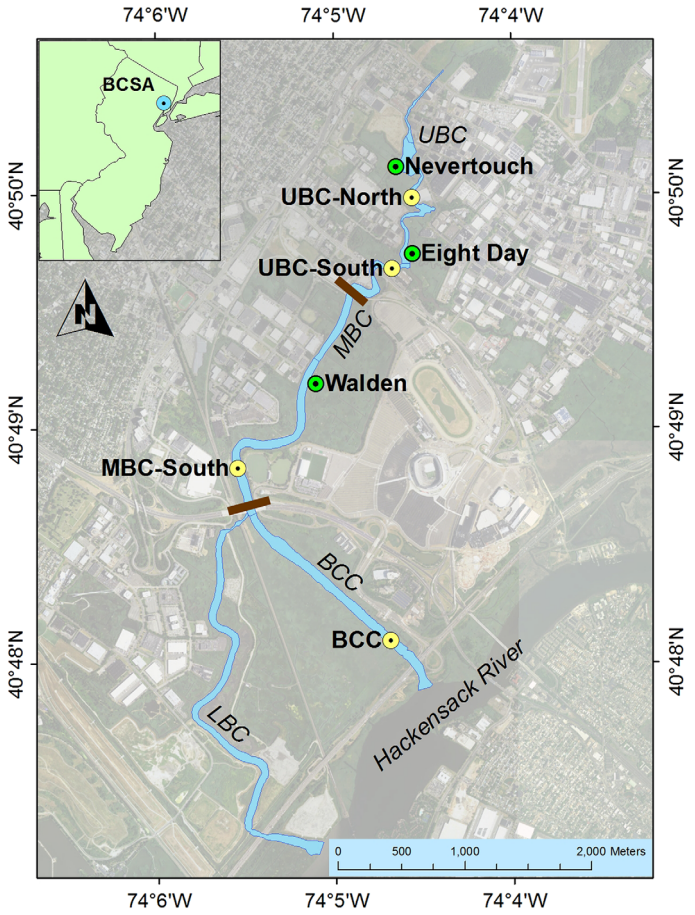


**Fig. 1.** The BCSA with four sections of the main waterway labeled in italics and separated by thick brown lines. Main channel water column study sites are indicated by yellow circles. Marsh tributary study locations are denoted by green circles. The inset shows the location of the BCSA in New Jersey, U.S.A.

the geomorphological components of the BCSA is key in planning for remediation of the site.

Typical of estuarine systems, water column concentrations of organic matter, suspended solids, and contaminants in the BCSA main channel and marsh tributaries vary temporally and spatially due to the tides, freshwater flow events, particulate resuspension and deposition dynamics, and interactions between marshes and waterways. Initial water column sampling within the BCSA demonstrated that adequate characterization of the full range of conditions throughout the system using conventional discrete water sampling is impractical due to the number of samples and locations that would need to be measured contemporaneously over time. The elucidation of chemical contaminant fate and transport requires sampling at a higher resolution than feasible with conventional discrete water sampling. Optically based methods developed by Bergamaschi et al. (2011) provide one approach to meeting this need.

Optically based chemical characterization is based on the premise that COCs have the tendency to preferentially adsorb onto organic particles and/or associate with dissolved organic material (e.g., Di Toro et al. 1991; McCarthy and Zachara 1998; Ullrich et al. 2001; Eggleton and Thomas 2004) that may have unique optical signatures. These optical signatures may describe particle composition (e.g., Twardowski et al. 2001; Sullivan et al. 2005; Chang et al. 2006), size distribution (e.g., Boss et al. 2001*a*,*b*; Agrawal and Mikkelsen 2009; Briggs et al. 2013), and/or concentration (Babin et al. 2003) including for colored dissolved organic matter (CDOM) (Coble et al. 2004); therefore optical measurements provide a potential means to quantify the concentration of COCs. Bergamaschi et al. (2011, 2012*a*,*b*) successfully developed and validated statistical models for the derivation of mercury and methyl mercury concentration from in situ optical properties and used the optically based results to quantify mass flux of mercury and methyl mercury throughout several different tidal estuaries. To the authors' knowledge, no previous studies have quantified concentrations of PCBs using in situ optical properties.

## Objectives

Two field studies using an OPTically-based In-situ Characterization System (OPTICS) were developed based on the pioneering work by Bergamaschi et al. (2011) to evaluate the sources and transport of COCs in the BCSA water column. The specific objectives were to: (1) evaluate the movement of suspended particulates and dissolved material in response to tidal action and moderate storm events and (2) quantify the exchange of COCs between the waterways and marshes.

## Methods

The 2014 OPTICS study was conducted over a month-long period covering one spring-neap tidal cycle in July. The 2015 OPTICS study encompassed two spring-neap tidal cycles from August to October. A wide range of environmental conditions (e.g., storms of differing magnitudes and variable salinity and water clarity) was encountered during the study periods.

### Study site description

The BCSA is a tributary of the Hackensack River estuary and includes 10 km of primary tidal waterway and 3 km$^2$ of marshes dominated by *Phragmites australis*. The main tidal channel, Berry's Creek, is well-mixed with no salt wedge observed in the system. Berry's Creek is separated into four main reaches: Lower Berry's Creek (LBC), Berry's Creek Canal (BCC), Middle Berry's Creek (MBC), and Upper Berry's Creek (UBC) (Fig. 1). UBC is relatively shallow (~ 2 m mean water depth), meandering, and narrow. The water deepens through MBC to BCC from about 4 m to greater than 5 m mean water depth. BCC is straight and wide and provides connectivity between the BCSA upper reaches and the Hackensack River out to Newark Bay and the Atlantic Ocean. LBC is also joined to the Hackensack River; however the primary connection between LBC and BCC is through a culvert, which highly

**Table 1.** Discrete water sample collection information for each sampling location. The number of discrete samples obtained for each analyte (including field duplicates) is in parentheses following each date of sample collection.

| | 2014 | | 2015 | |
|---|---|---|---|---|
| Location | Calibration | Validation | Calibration | Validation |
| MBC-south | 13 Jul (18) | 01 Jul (18) | 31 Aug (17) | 11 Sep (8)* |
| | 25 Jul (18) | | 22 Sep (17) | 20 Oct (10) |
| | | | 30 Sep (21)† | 29 Oct (10) |
| UBC-south | 13 Jul (18) | 01 Jul (18) | 31 Aug (17) | 11 Sep (8)* |
| | 25 Jul (18) | | 22 Sep (17) | 20 Oct (10) |
| | | | 30 Sep (21)† | 29 Oct (10) |
| Nevertouch Marsh | — | — | 30 Aug (16) | 25 Sep (8) |
| | | | 23 Sep (17) | |
| Eight Day Swamp | — | — | 30 Aug (17) | 25 Sep (8) |
| | | | 23 Sep (17) | |
| Walden Swamp | — | — | 29 Sep (17) | 28 Oct (10) |
| | | | 19 Oct (16) | |

*Rain event.
†Storm sampling to capture changes in flow conditions.

restricts flow between the two reaches. As a result, LBC is not considered here.

The lower reaches of the BCSA are characterized by average water residence times on the order of 1 d due to routine tidal exchange with the river, while the more distant UBC and the northern end of MBC are less frequently exchanged and characterized by average water residence times of 3–6 d (BCSA Group 2018). The middle and lower portions of MBC are a mixing zone for uplands-derived freshwater flow and estuarine flow derived from tidal exchange with the Hackensack River.

Flow and transport throughout the BCSA are dominated by semi-diurnal tidal oscillations, which can be interrupted by freshwater flow during storm events. Average flow rates are generally low (less than 30 $m^3/s$) in the UBC and increase to near 150 $m^3/s$ in BCC at the confluence with the Hackensack River (BCSA Group 2018). Larger storm events can increase system-wide flow rates by up to 200%. Upland flow to the tidal area is generally confined to storm drainages. Flow at the head of the system in UBC is bounded by tide gates, which limit upland tidal flooding. Tidal processes result in routine inundation of the *Phragmites* marshes and greatly influence the fate and transport of sediment and biogeochemical constituents within the system.

The *Phragmites* marshes are an important contributor to organic material to the system. Degradation of this organic matter leads to an abundance of detritus and fines in the system and the prevalence of an unconsolidated benthic layer, or "fluff layer." The fluff layer has been observed in sediment profile images and cores collected throughout the BCSA main channel (BCSA Group 2012). The fluff layer is typical in estuarine systems, is generally less than 1 cm thick, interacts with the underlying sediment bed, and is susceptible to resuspension and deposition processes (e.g., Curran et al. 2007; Fugate and Friedrichs 2003; Lick 2009).

**Discrete water samples**

Discrete water samples were collected in several BCSA main channel and marsh tributary locations for laboratory-based COC analysis to statistically relate to the near-continuous, high temporal resolution in situ optical and water quality data, following methods described by Bergamaschi et al. (2011). Main channel discrete water samples were collected at fixed moored hydro-stations in MBC-south and UBC-south, and marsh tributary samples were collected at Nevertouch Marsh and Eight Day Swamp in UBC and Walden Swamp in MBC (Table 1; Fig. 1). Samples were obtained hourly (or half-hourly at marsh tributaries following slack low tide), concurrently with in situ measurements (described below) over several 6-h or 12-h sampling periods in 2014 and 2015 (Table 1) for laboratory determinations of filtered (dissolved) and unfiltered mercury and methyl mercury (FHg, UHg, FMeHg, and UMeHg) and unfiltered PCBs (UPCBs). Dissolved PCBs had previously not been detected at the study site; therefore, only UPCBs were considered. Particulate concentrations of discrete sample Hg and MeHg were determined by difference (unfiltered minus filtered; PHg and PMeHg). Water samples were also analyzed for total suspended solids (TSS). TSS was measured using standard method SM 2540D (Greenberg et al. 1992). Unfiltered and dissolved Hg and MeHg concentrations were determined following USEPA methods 1631E (USEPA 2002) and 1630, respectively, and UPCBs were analyzed using USEPA method 8082. See United States Code of Federal Regulations 40 CFR Part 136 (http://www.epa.gov/cwa-methods) for more information. Discrete sample data collection and analysis followed a detailed quality assurance project plan, which is included in the USEPA public records for the study site, as well as USEPA protocols for laboratory quality assurance, certification, and validation processes that are inherent to CERCLA investigations.

All water samples were collected by peristaltic pump through sterile sampling tubes with intakes located at the same elevation as the in situ optical and water quality sensors. Samples for dissolved constituents utilized a high capacity capsule filter with 0.45 $\mu$m pore size. A total of 54 samples of each analyte was collected at each of the MBC-south and UBC-south locations in 2014; 83 samples were collected at each of the main channel monitoring locations in 2015 and at least 40 discrete samples were collected at each of the marsh tributary locations, including field duplicates (Table 1). One-third of all discrete samples collected consisted of field duplicates.

## In situ measurements

### *Main channel instrumentation*

In 2014, four main channel waterway locations were equipped with suites of optical and physical sensors on fixed piling moored hydro-stations in BCC, MBC-south, UBC-south, and UBC-north (Fig. 1). Discrete water samples were collected at the MBC-south and UBC-south stations. Laboratory-based TSS data are available at all monitoring stations; discrete COC samples were not collected at BCC or UBC-north. In 2015, the fixed piling moored hydro-stations in MBC-south and UBC-south were instrumented. The sensor suites included the following instrumentation: WET Labs (Philomath, Oregon) ECO-fluorometers for CDOM and chlorophyll *a* concentration (Chl *a*); WET Labs ECO-backscatter sensor for particulate backscattering coefficient at 660 nm ($b_{bp}$); and YSI (Yellow Springs, Ohio) water quality sonde with probes for conductivity, temperature, depth, and turbidity. The YSI water quality sensor sampled every 15 min starting on the hour and ECO sensors burst sampled for 30 s every 15 min starting on the hour. The flat-faced optical ECO sensors and YSI water quality probes were equipped with anti-biofouling measures for long-term deployments. The measurement windows of all optical sensors in 2014 were located at distances of 2.66 m, 1.37 m, and 0.4 m above the sediment bed for systems at BCC, MBC, and UBC locations, respectively. The measurement depth was 0.6 m above the sediment bed in 2015.

Ancillary measurements of water column current velocity and direction at 0.25 m vertical bins were provided by acoustic Doppler current profilers (ADCPs; Teledyne RD Instruments 1200 kHz Workhorse Sentinel, Poway, California) that were deployed uplooking on bottom-mount platforms at moored monitoring hydro-stations. ADCPs were programmed to sample every 15 min. Additionally, in 2014, high-resolution single-point current meters (Sontek, ADVOcean-Hydra; San Diego, California) were deployed near-bed at MBC-south and UBC-south to characterize bottom shear stress. These sampled at 25 Hz for 10 min every 30 min. Moored hydro-station instruments were deployed between 01 July and 30 July in 2014 and between 29 August and 30 October in 2015.

### *Marsh tributary instrumentation*

Month-long marsh tributary studies were conducted at three different locations in 2015 to investigate marsh-waterway dynamics. Nevertouch Marsh, Eight Day Swamp, and Walden Swamp tributaries (Fig. 1) were each equipped with an ADVOcean-Hydra, ECO-fluorometers for CDOM and Chl *a*, ECO-backscattering sensor, and YSI water quality sonde. Sensors were bottom-mounted and placed in the center of the tributary channel (i.e., in the thalweg) such that measurement areas were ~ 0.2 m above the sediment bed and not obscured by channel banks or large debris. The sampling rates of optical and water quality sensors remained unchanged from those employed during the main channel study; the ADVOcean-Hydra sampling rate was increased to 25 Hz for 10 min every 15 min. Instrumentation suites were initially deployed at Nevertouch Marsh and Eight Day Swamp on 29 August 2015 and finally recovered on 28 September 2015. Following recovery, sensors were cleaned and calibrations were verified, and all batteries were assessed and replaced as necessary. An entire suite of instrumentation was then redeployed at Walden Swamp on 29 September 2015. This system was finally recovered on 29 October 2015.

### *Instrument calibrations and data processing*

All sensors were calibrated prior to deployment and data were analyzed after recovery following manufacturer-recommended protocols and optical analysis methods from the literature (Boss and Pegau 2001; Zhang et al. 2009; Slade and Boss 2015). The YSIs were calibrated to National Institute of Standards and Technology (NIST) standards. All ECO sensors were corrected to dark count calibrations conducted prior to deployment. Optical and physical data were burst-averaged and merged with the YSI data set such that all data streams had the same time stamp. The exception was the main channel near-bed ADVOcean-Hydra deployed in 2014, which sampled every 30 min. Near-bed shear stress was derived from ADVOcean-Hydra data following methods outlined by Kim et al. (2000).

## OPTICS statistical regression model

Following methods introduced by Bergamaschi et al. (2011), partial-least squares (PLS) regression (de Jong 1993; Rosipal and Krämer 2006) was utilized to statistically correlate the laboratory-analyzed discrete sample COC data to high temporal resolution in situ water quality and optical data streams. PLS regression combines multiple linear regression and principal component analysis (PCA), where multiple linear regression finds a combination of predictors that best fit a response and PCA finds combinations of predictors with large variance. Therefore, PLS identifies combinations of multicollinear predictors (here, optical and water quality properties) that have large covariance with the response values (here, COC analytical data). PLS combines information about the variances of both the predictors and the observations while also considering the correlations among them. PLS therefore provides a model with reliable predictive power.

The OPTICS PLS model was developed and executed in MATLAB® (The MathWorks) for the following response variables: FHg, UHg, PHg, FMeHg, UMeHg, PMeHg, as well as

UPCBs. Particulate components of Hg and MeHg were determined by both the PLS model and by difference (i.e., modeled unfiltered minus modeled filtered) to confirm consistency. Station-specific OPTICS PLS regressions were developed for each of the study years, 2014 and 2015, independently. PLS regressions were optimized to maximize the variance explained between predictors and responses while reducing residuals or error, without model over-constraint, which was defined as negative concentration values and/or unnatural "spikiness" in derived quantities, e.g., rapid increases and/or decreases in COC concentrations over time scales of a couple of hours or less. Site-specific OPTICS regression utilized a model calibration data set and each OPTICS model was validated with an independent data set (Table 1). Field duplicates for discrete samples were averaged.

The suites of predictor variables for OPTICS studies included in situ measurements of water quality and optical properties: water depth, temperature, salinity, turbidity, particulate backscattering coefficient, and CDOM and Chl *a* concentration derived from fluorescence. The selection of optical and water quality predictors was based on the results of the study presented by Bergamaschi et al. (2011), as well as prior assessments of optical responses to particulates and dissolved material in the BCSA (BCSA Group 2010, 2012). Predictor data sets were constructed by selecting optical and water quality measurements conducted at the same times as the discrete sample collection. High resolution, station-specific time series of TSS were derived through traditional least-squares linear regression between in situ measurements of optical turbidity and TSS determined from discrete samples.

**Marsh COC flux analysis**

The primary focus of the 2015 OPTICS marsh tributary monitoring program was to evaluate the exchange of dissolved and particulate COCs between the marshes and waterways in relation to system processes such as routine tidal flooding and drainage of the BCSA marshes and storm flows. Quantitative marsh exchange analysis involved calculation of instantaneous mass fluxes of COCs ($F_{COC}$; 15-min intervals), net daily mass flux of COCs ($M_1$), and total and relative daily marsh mass exchange ($M_T$ and $M_R$, respectively) at each marsh tributary location monitored in 2015. Instantaneous mass flux is the product of concentration and flow rate:

$$F_{COC} = Q_t \times C_t \quad (1)$$

where $Q_t$ is flow rate, $C_t$ is COC concentration determined from the OPTICS regression model, and the subscript $t$ represents time-dependence. Flow rate at monitored marsh tributaries was computed following:

$$Q_t = U_t \times A_t \quad (2)$$

where $U_t$ and $A_t$ are along-channel velocity and channel cross-sectional area, respectively, at time $t$. Cross-sectional areas at each marsh tributary monitoring location were computed as a function of water level based on a digital elevation model (BCSA Group 2018) and in situ measurements of water depth. Along-channel velocity was derived from moored ADVOcean-Hydra current velocity measurements. Due to the shallow water depths (< 3 m mean sea level to completely dry), no cross-channel or depth-resolved current velocity data were available; therefore the following assumptions were made for estimates of $U_t$: (1) current velocities measured at a single depth 0.2 m above the sediment bed were representative of water column velocities and (2) current velocities measured at a single cross-channel location, in the thalweg, were representative of along-channel velocities. Downstream flow and flux (ebb tide) were defined as positive and upstream flow and flux (flood tide) as negative. In order to eliminate directional biases from along-channel velocity uncertainties, the assumption of zero net volume of flow over each tidal cycle (~ 25 h) was made, i.e., water volume into the tributary equaled water volume out. The marsh tributary monitoring locations are primary drainages and near to the main channel (Fig. 1), thus justifying this assumption of zero net tidal flow volume.

Net daily mass flux ($M_1$) was determined by integrating $F_{COC}$ over each tidal day, $T$ (~ 25 h) (Eq. 3). Data collected when marsh tributary water depths were less than 0.2 m were excluded from this calculation to ensure that flux data were derived from measurements taken when sensors were fully submerged. Total daily marsh mass exchange, $M_T$, is the total amount of material advected through the monitored marsh tributary, assumed to be the total amount of mass exchanged between the marsh and waterway in either direction (Eq. 4). The relative daily marsh mass exchange, $M_R$, is an indication of flood-dominant or ebb-dominant marsh exchange, suggestive of waterway-to-marsh transport (negative values) or marsh-to-waterway transport (positive values) (Eq. 5).

$$M_1 = \int_0^T (Q_t \times C_t)\, dT \quad (3)$$

$$M_T = \int_0^T |\, (Q_t \times C_t)\, |\, dT \quad (4)$$

$$M_R = 100^* M_1 / M_T \quad (5)$$

Following the calculation of instantaneous, net daily, total daily, and relative daily COC fluxes, the average of net daily mass flux over the marsh tributary monitoring periods was taken to represent average daily mass exchange between marsh and waterway for each marsh location and each COC. Error bars were derived from average percent differences between modeled and measured COC concentrations (i.e., assumed zero error in the water balanced flow rate), or:

$$\text{Percent Difference} = \overline{100 \times \left[ \frac{(COC_{OPTICS} - COC_{lab})}{COC_{lab}} \right]} \quad (6)$$

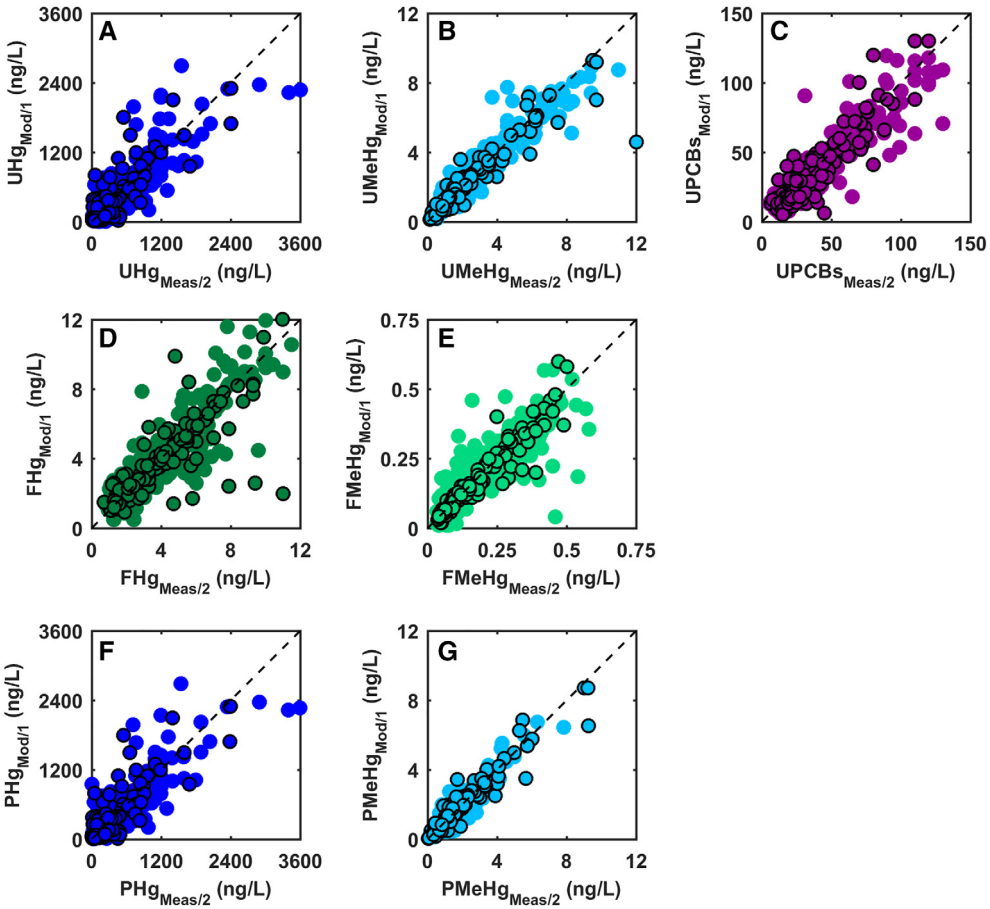


**Fig. 2.** Linear regression between OPTICS-derived (modeled) and discrete sample (measured) data (solid filled circles) and between discrete sample field duplicates (outlined in black) for (**A**) UHg, (**B**) UMeHg, (**C**) UPCBs, (**D**) FHg, (**E**) FMeHg, (**F**) PHg, and (**G**) PMeHg for data collected at MBC-south, UBC-south, Nevertouch Marsh, Eight-Day Swamp, and Walden Swamp in 2014 and 2015 combined. The 1 : 1 line (dashed) is provided.

where $COC_{OPTICS}$ represents OPTICS modeled COC data, $COC_{lab}$ indicates discrete water sample data, and the overbar indicates the mean.

## Results

The 2014 and 2015 studies confirmed and augmented the work presented by Bergamaschi et al. (2011) by showing that the OPTICS approach is a robust and reliable method of obtaining high temporal resolution measurements of unfiltered, filtered (dissolved), and particulate COC concentrations. Importantly, OPTICS studies afforded the ability to investigate transport and exchange of COCs throughout the BCSA. OPTICS monitoring covered a complete range of tidal conditions and several precipitation events, which are key processes that affect the variability of COCs and optical and water quality parameters.

### COC concentrations estimated from OPTICS

OPTICS-derived (modeled; Mod) vs. discrete sample data (measured; Meas) statistical comparisons of five different COCs (filtered and unfiltered mercury and methyl mercury and unfiltered PCBs) at five monitoring locations (two main channel and three marsh tributaries) over two monitoring years were conducted with all locations and years combined (Fig. 2—includes PHg and PMeHg; Table 2). Goodness of fit ($R^2$) was determined through least-squares linear regression analysis. Median ratio (Ratio), mean absolute bias (Bias), root-mean-square error (RMSE), and error (Residuals) were calculated following:

$$\text{Ratio} = \text{median}\,(\text{Mod}/\text{Meas}) \tag{7}$$

$$\text{Bias} = \text{mean}\,(\,|\,\text{Mod} - \text{Meas}\,|\,) \tag{8}$$

$$\text{RMSE} = \sqrt{\text{MSE}} \tag{9a}$$

$$\text{MSE} = \overline{(\text{Mod-Meas})}^2 \text{ (the overbar indicates the mean)} \tag{9b}$$

$$\text{Residuals} = \text{Mod} - \text{Meas} \tag{10}$$

Modeled vs. measured statistical metrics were compared to the same metrics computed between discrete field sample duplicates ($D_1$ and $D_2$ substituted for Mod and Meas in Eqs. 7

**Table 2.** Results of statistical analysis of OPTICS-derived (modeled) vs. discrete field samples (measured) data for all monitoring locations and study years combined (discrete sample field duplicate statistical metrics are indicated in parentheses). *N* = number of samples, $R^2$ = coefficient of determination, Ratio = median ratio, Bias = mean absolute bias, and RMSE = root mean square error (Eqs. 7–9).

| Constituent | *N* | $R^2$ | Ratio | Bias | RMSE |
|---|---|---|---|---|---|
| FHg | 306 (126) | 0.77 (0.61) | 1.03 (1.0) | 0.74 (0.72) | 1.07 (1.48) |
| UHg | 307 (126) | 0.79 (0.69) | 1.01 (0.97) | 148 (148) | 252 (250) |
| FMeHg | 294 (121) | 0.75 (0.96) | 1.01 (1.0) | 0.05 (0.03) | 0.09 (0.05) |
| UMeHg | 304 (125) | 0.91 (0.85) | 0.99 (1.0) | 0.39 (0.36) | 0.61 (0.84) |
| UPCBs | 307 (126) | 0.83 (0.81) | 0.97 (1.03) | 7.64 (8.23) | 11.4 (11.4) |

through 10) to evaluate the reliability of the OPTICS PLS regressions (Table 2; Residuals not provided). Extensive statistical metrics were also developed separately for waterway and marsh locations, discrete sampling date, and by study year and are comparable to metrics computed for the entire data set. These metrics not presented here but were evaluated as part of a BCSA OPTICS study peer review conducted by the USEPA.

In general, statistical results indicated excellent overall model performance. $R^2$ values exceeded 0.75, Ratios were within $\pm$ 0.03 of 1.0, and Bias and RMSE values were low (Bias generally within 0.75 ng/L and RMSE within 1.1 ng/L), with the exception of UHg and UPCBs, which showed higher Bias (148 for UHg and 7.6 for UPCBs). Maximum model residuals (Eq. 10), or error, for each COC were generally within 25% of measured quantities and model residual quantities were similar to or lower than discrete field sample duplicate residuals (data not shown). Model and field duplicate residuals were normally distributed, indicating random error, i.e., there is no discernable pattern in environmental conditions in which the model fits well or does not fit well. Statistical metrics computed for discrete field duplicates (i.e., the training data set) and for modeled vs. measured data (i.e., the test data set) were comparable, indicating that the OPTICS PLS regression produced results that generally exhibited a lower or similar degree of variance compared with discrete field sample duplicates.

The goodness of fits between modeled and measured COCs were generally in agreement with those presented by Bergamaschi et al. (2011) for data collected in the San Francisco Bay estuary (Browns Island). Bergamaschi et al. (2011) reported $R^2$ of 0.96, 0.79, and 0.50 for FMeHg, UMeHg, and PMeHg, respectively. The San Francisco Bay study utilized the entire analytical dataset with a step-wise sample exclusion routine for model cross-validation. Here, comparable correlation coefficients are reported despite the use of fully independent validation datasets. These statistical metrics support the validity of OPTICS as a predictive tool.

## Main channel variability related to tidal and storm processes

### *Particulate matter*

The strongest variability in time series observations at main channel monitoring locations was associated with the spring-neap tidal signal and semi-diurnal tidal oscillations (Fig. 3). As expected, tidal excursions and salinity were greater during spring tide conditions (e.g., 13 July 2014). Current velocity throughout the water column as well as near-bed shear stress was stronger during spring tide as compared to neap tide, also as expected. At all main channel stations and both years of monitoring studies (2015 not shown), elevated TSS and concentrations of derived particulate COCs were also observed nearest to spring tide periods, coinciding with higher current velocity and near-bed shear stress, which is suggestive of sediment and particulate-bound COC resuspension processes (Fig. 3).

Under dry weather conditions, evidence of resuspension processes were observed across the semi-diurnal tidal cycle, in which increases in TSS and concentrations of particulate COCs and UPCBs coincided with maximum flood and ebb tidal velocities (Fig. 4A). TSS and concentrations of particulate COCs and UPCBs were observed to decline during low velocity periods around high and low slack tides (Fig. 4A), suggesting that a portion of the water column particulates and associated COCs settled to the sediment bed during these low energy periods. Particulate COCs, UPCBs, and TSS concentrations varied on the order of twofold to 10-fold over the course of the tidal cycle, with a greater overall difference observed during spring tide conditions compared to neap tide conditions. These observations are consistent with near-bed monitoring conducted in the BCSA main channel showing that low-density particulates are resuspended from the fluff layer at the surface of the sediment bed (upper ~ 5 mm) during peak tidal velocities and deposited during lower velocity periods (BCSA Group 2018).

Routine semi-diurnal tidal oscillations over the OPTICS study monitoring periods were interrupted by precipitation events: two storms in 2014 (02 July–03 July and 13 July–14 July; Fig. 3) and three rain events in 2015 (10 September–11 September, 29 September–03 October, and 28 October; not shown). The storm event on 02 July 2014 and 03 July 2014 resulted in 7 cm of precipitation during two intense rainfall periods over a span of 28 h. This storm resulted in a large influx of freshwater to the BCSA, particularly in the upper reaches (Fig. 3). Salinity in UBC dropped to nearly zero ppt

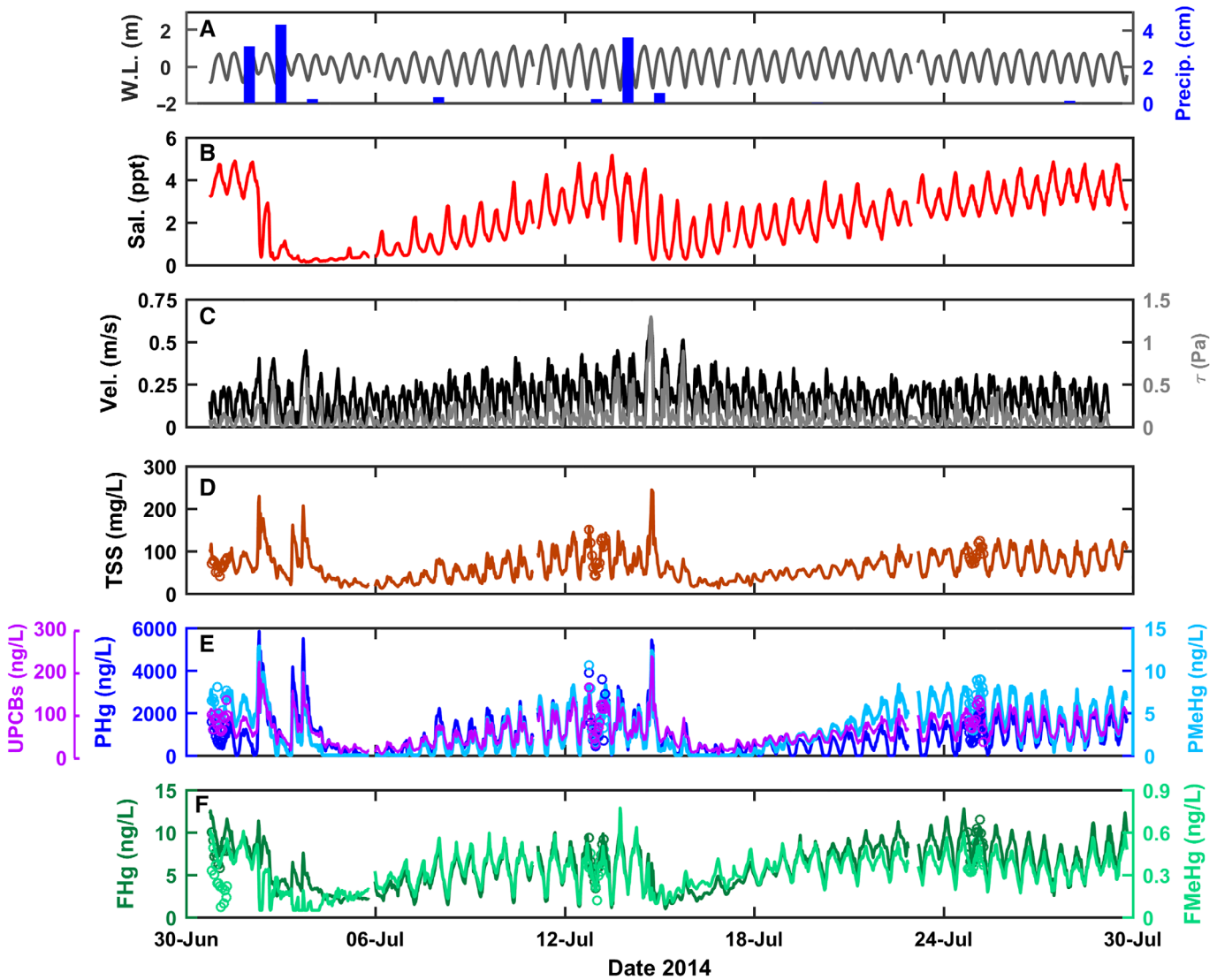


**Fig. 3.** In situ water quality and hydrodynamics data and OPTICS-derived COCs at UBC-south in 2014. Discrete sample data are shown with open circles. (**A**) Water level (referenced to mean sea level; W.L.) and precipitation (from Teterboro Airport, NJ; Precip.), (**B**) salinity (Sal.), (**C**) current velocity (Vel.) and shear stress ($\tau$), and concentration of (**D**) total suspended solids (TSS), (**E**) particulate COCs (and UPCBs), and (**F**) dissolved COCs. High uncertainties in FMeHg field duplicate samples during water sampling on 01 July 2014 resulted in discrepancies between modeled and measured FMeHg (panel **F**). Time series gaps are during instrumentation servicing periods.

and did not recover to pre-storm conditions for nearly 1 week. Water column and near-bed current velocities recorded in UBC during the period of maximum freshwater inflow were nearly double the value of pre-storm tidal velocities. This resulted in sharp, short-term increases in TSS, particulate COCs, and UPCBs (peaks of 2–5 times the average, pre-storm concentrations), likely due to sediment and particle-bound COC resuspension processes, before rapidly declining to less than half of pre-storm levels and remaining at relatively low levels for several days following the storm (Figs. 3–4B). The range in tidally driven fluctuations in TSS, particulate COC, and UPCB concentrations were diminished during this several day period compared to pre-storm conditions. Within about 1 week, TSS, particulate COCs, and UPCBs were observed to have returned to pre-storm levels and the tidal oscillation patterns were re-established at UBC (Fig. 3). These storm-induced effects described for UBC were observed, to a lesser extent at MBC-south, but had limited effect at the BCC monitoring location (Fig. 5). The semi-diurnal tidal oscillations continued in MBC and BCC throughout and following the storm period. BCC physical, water quality, and optical properties were relatively unaffected by the 02 July 2014–03 July 2014 storm except a decrease in salinity (Fig. 5).

Similar though more subdued responses were evident during smaller magnitude storms that influenced the BCSA during the 2014 and 2015 OPTICS monitoring studies (Fig. 3;

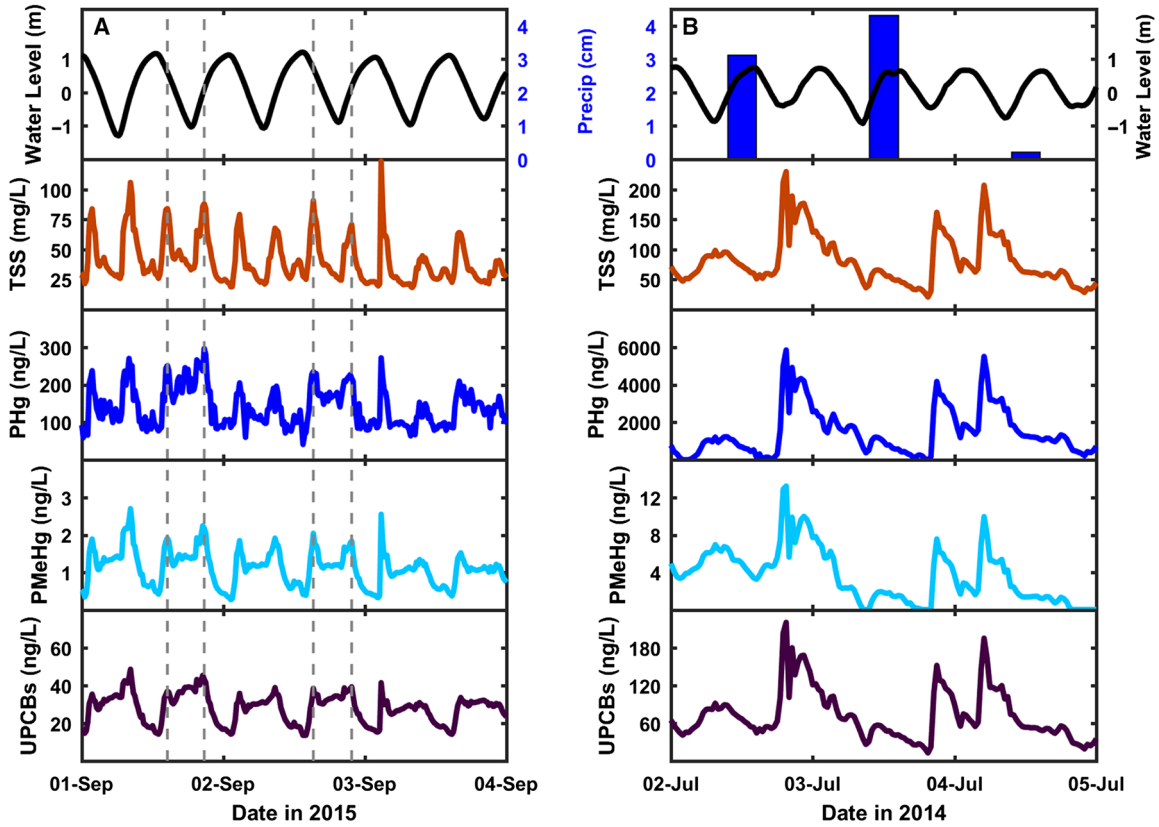


**Fig. 4.** Three-day time series of water level (referenced to mean sea level) and precipitation (blue bars), TSS, PHg, PMeHg, and UPCBs during (**A**) dry conditions at MBC-south in 2015 illustrating observed tidal oscillations and particulate responses (select peak ebb and flood tide periods are denoted with dashed lines) and (**B**) the 02 July 2014–03 July 2014 storm at UBC-south illustrating sharp increases in particulate COCs and UPCBs due to precipitation events and high flow.

2015 data not shown). These observations were consistent with the smaller runoff volume associated with these storms and the lesser influence of the runoff from these storms on channel velocities in the BCSA waterway.

Mercury concentrations at BCSA are on average higher than those found in other tidal estuaries in the U.S. Mason et al. (1999) reported Chesapeake Bay surface water THg concentrations to be generally less than 10 ng/L and lower than 3 ng/L in non-urbanized regions. In San Francisco Bay estuary, California, David et al. (2009) reported THg concentrations ranging between 3.2 ng/L and 75 ng/L (Mallard Island) and Bergamaschi et al. (2011) presented TMeHg concentrations between ~ 0.02 ng/L and 0.22 ng/L (Browns Island).

### *Dissolved material*

The temporal patterns in OPTICS-derived dissolved COCs also reflected tidal oscillations in the system (Figs. 3, 6A). Dissolved COCs increased during ebb tide periods and reached a maximum at slack low tide, then decreased with the flood tide and reached a minimum value at slack high tide (Fig. 6A). These patterns suggest a north to south (UBC to BCC) gradient of decreasing COC concentration across the BCSA (Figs. 3, 5) and tidally driven movement of water back and forth within the system.

The pattern in dissolved COC concentrations in response to storms was similar to that observed for salinity, where concentrations decreased on the order of 2–5 times at UBC with the influx of storm runoff (Figs. 3, 6B). Dissolved COC concentrations showed a decreasing storm influence with distance downstream, with lesser influence of the storm flows on dissolved chemical constituents at MBC-south (Fig. 5).

### Marsh exchange processes

The 2015 OPTICS monitoring program was designed to augment the understanding of COC exchange dynamics between the marsh and waterway through estimation of COC mass fluxes between the waterways and marshes during tidal inundation and freshwater flow events. Multiple lines of evidence collected during the BCSA remedial investigation (RI) program indicated that there is net transport of particulates and particulate-phase COCs from the waterway to the marshes (BCSA Group 2018). Similar to other tidal marsh systems, the BCSA marshes are net depositional (e.g., Dyer 1997; Friedrichs and Perry 2001; Friedrichs 2011). Characterization of marsh pore-water quality and marsh hydrologic properties during the RI program suggested that, although

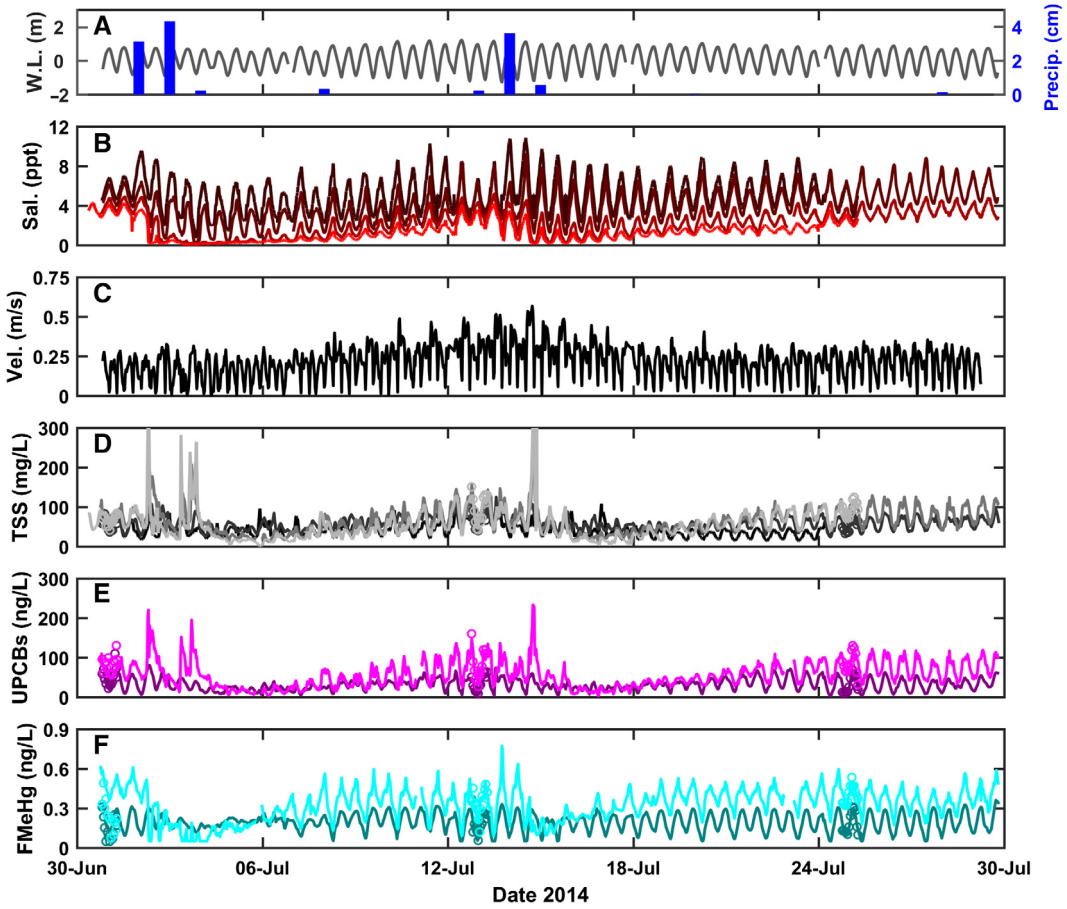


**Fig. 5.** OPTICS study data from 2014. Discrete sample data are shown with open circles. (**A**) Water level at MBC-South (referenced to mean sea level; W.L.) and precipitation (from Teterboro Airport, NJ; Precip.); (**B**) salinity (Sal.) at all four monitoring stations; (**C**) current velocity (Vel.) at MBC-South; (**D**) total suspended solids (TSS) at all four stations; and (**E**) UPCBs and (**F**) FMeHg at MBC-South and UBC-South. Darker to lighter colors represent data from the lowest reach, BCC, to the uppermost station in UBC. Time series gaps are during instrumentation servicing periods.

there is a potential for transport of FHg and FMeHg from the marshes to the waterway, this transport accounts for less than 10% of total COC mass flux and is not significant to BCSA water quality (BCSA Group 2018).

With the exception of Nevertouch Marsh, marsh COC mass exchange analysis results showed a slight export of FHg and FMeHg from the marshes and substantial import of PHg, PMeHg, and UPCBs into the marshes (Table 3; Figs. 7–8). The export of FHg and FMeHg from Eight Day Swamp tributary accounted for less than 0.2% and less than 5% of UHg and UMeHg mass exchange, respectively. This signifies that over 95% of Eight Day Swamp mass exchange was the import of PHg and PMeHg from the waterway (Table 3). Walden Swamp results were similar; FHg and FMeHg export was less than 0.5% and less than 7% of UHg and UMeHg mass exchange; particulate import was over 99% and 93% of unfiltered Hg and MeHg mass, respectively (Table 3). Nevertouch Marsh tributary results indicated mass exchange of FHg, FMeHg, PHg, and PMeHg from the waterway into the marsh, likely the result of northern UBC recirculation.

To verify marsh exchange findings based on OPTICS model-derived COC concentrations, COC mass fluxes were calculated with discrete water sample data collected at Nevertouch Marsh and Eight Day Swamp. Walden Swamp data were excluded from this analysis because the discrete water sampling period did not encompass an entire ebb-flood tidal cycle. The results of mass flux calculations based on the 30 August 2015 discrete water sample data sets for Nevertouch Marsh and Eight Day Swamp tributaries were similar to those obtained using OPTICS-derived data. Discrete sample mass flux analysis showed net mass transport of particulate COCs into the marshes (Table 4). Further, limited transport of dissolved COCs was found between Nevertouch Marsh and Eight Day Swamp tributaries and the waterway; FHg mass flux was less than 1% of the PHg mass flux and FMeHg mass flux was between 3% and 6% of the PMeHg mass flux. These findings are consistent with other RI lines of evidence that indicate import of particulate COCs from the waterway to marshes and that transport of dissolved COCs from the marshes to the waterway was small relative to the mass transport of particulate COCs into the marshes.

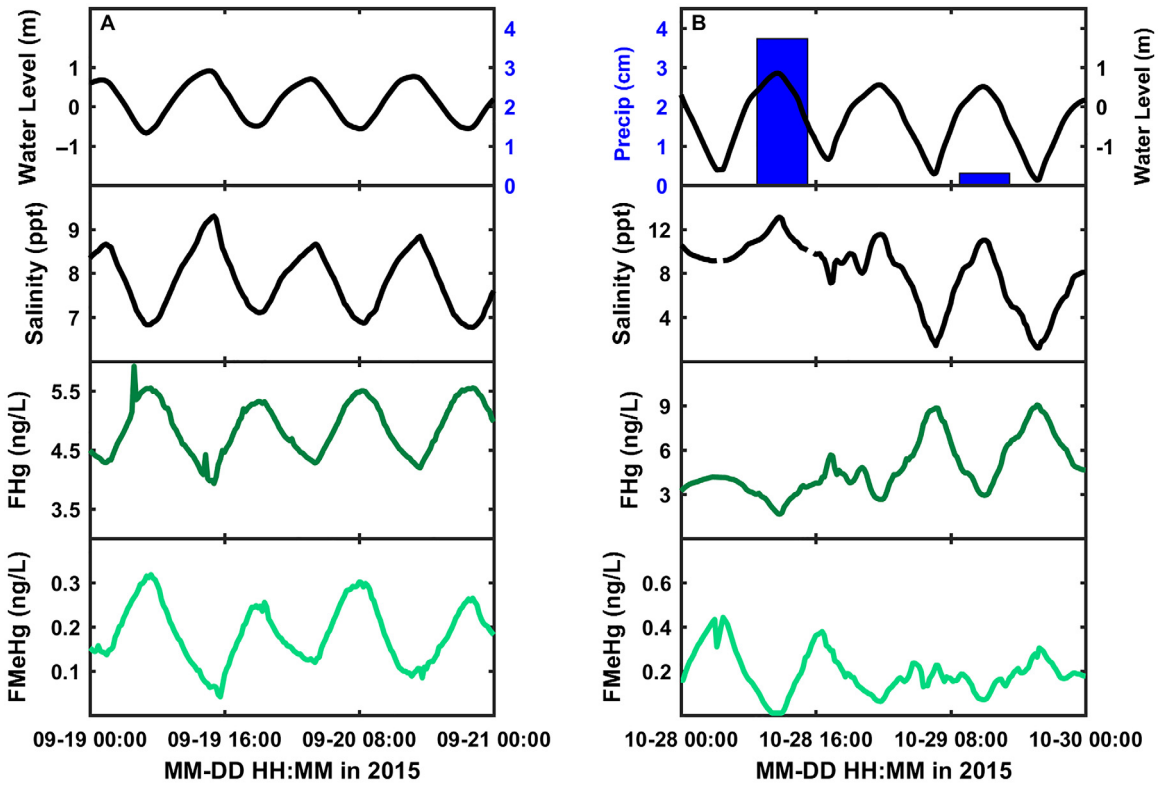


**Fig. 6.** Two-day UBC-south time series of water level (referenced to mean sea level) and precipitation (blue bars), salinity, FHg, and FMeHg during (**A**) dry conditions in 2015 illustrating observed tidal oscillations in dissolved COCs, and (**B**) 28 October 2015 rain event illustrating a decrease in dissolved COCs during precipitation events.

## *Discussion and conclusions*

A high-resolution OPTICS monitoring program utilized commercial off-the-shelf in situ optical and water quality sensors and a statistically based model prediction technique (following Bergamaschi et al. 2011) to derive high-frequency measurements of COC concentrations at multiple locations in the BCSA waterway and marshes over several spring-neap tidal periods. High temporal resolution time series of COC concentrations enabled characterization of water column contaminant dynamics throughout the BCSA. OPTICS provided observations of suspended particulates in response to tidal action and storm events in the main waterway, as well as data necessary for quantification of marsh-waterway exchange of COCs.

### Conceptual site model (CSM)

Based on results from OPTICS monitoring studies and corroborated with multiple lines of evidence determined from the BCSA RI program (BCSA Group 2018), it was determined that the BCSA main channel sediments are the primary ongoing source of COC mass to the water column. High organic content particulates, primarily derived from *Phragmites* marsh production, deposit to the main channel sediment bed during slack tides to form a thin veneer of low-density, unconsolidated material on the surface of the main channel sediment bed (Fig. 9A). COCs are potentially exchanged from main channel bedded sediment to these organic particulates in the fluff layer of the sediment surface (Fig. 9B). Resuspension of

**Table 3.** Net daily mass flux averaged over the monitoring period for dissolved and particulate COCs and UPCBs derived from OPTICS marsh tributary monitoring studies conducted in 2015. The percent contribution of particulate COC to unfiltered COC exchange is indicated in parentheses for Hg and MeHg.

| Location | PHg (mg) | PMeHg (mg) | UPCBs (mg) | FHg (mg) | FMeHg (mg) |
|---|---|---|---|---|---|
| Nevertouch Marsh | −7431 (99.6%) | −23 (97.0%) | −326 | −30 | −0.7 |
| Eight Day Swamp | −1301 (99.8%) | −1.9 (95.2%) | −21 | 2.3 | 0.1 |
| Walden Swamp | −1805 (99.5%) | −13 (93.1%) | −79 | 9.0 | 0.9 |

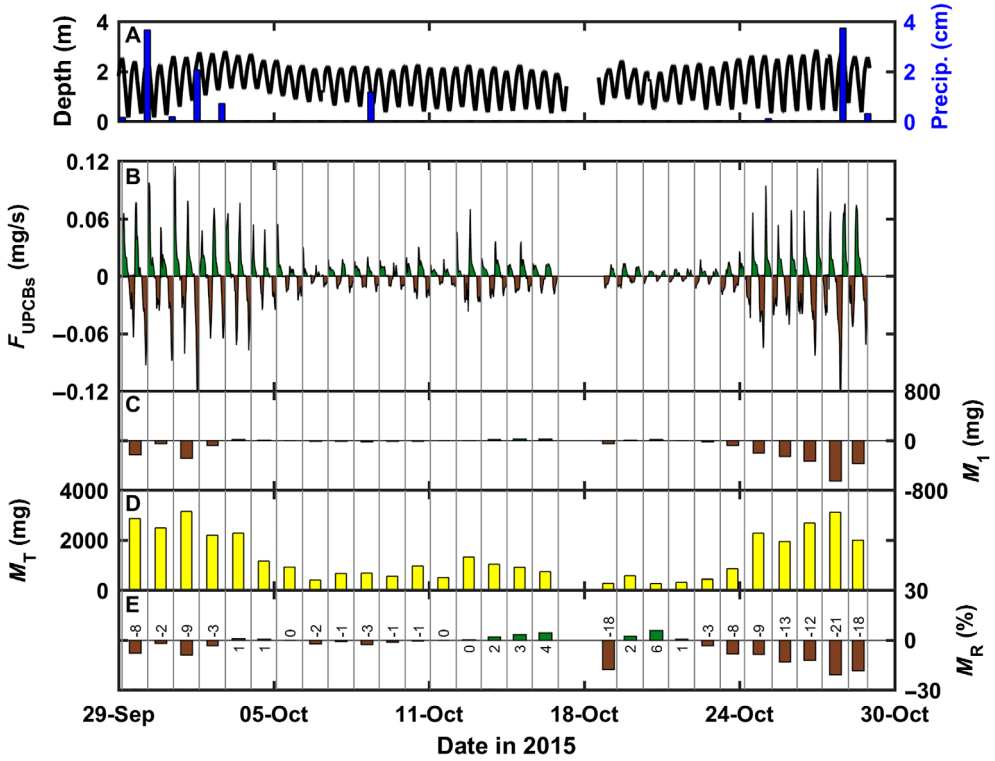


**Fig. 7.** Results from marsh exchange analysis for UPCBs at Walden Swamp tributary: (**A**) water depth and precipitation (shown for context), (**B**) instantaneous mass flux of UPCBs ($F_{UPCBs}$), (**C**) net daily mass flux ($M_1$), (**D**) total daily mass exchange ($M_T$), and (**E**) relative daily mass exchange ($M_R$). See text for computations. Mass fluxes from marsh-to-waterway are positive and shown in green and fluxes from waterway-to-marsh are negative and shown in brown. Gray vertical lines delineate tidal days ($T$; ~ 25 h). Note that fluxes calculated for the period following instrumentation servicing (18 October) were not over an entire tidal day and therefore may be biased.

these particulates by tidal action and storm flows is likely an important mechanism of COC exchange from the main channel sediment to the water column (Fig. 9C). COCs associated with resuspended particulates are transported from the main channel waterway to the marshes, where they are retained (Fig. 9D). As quantified in Tables 3–4 and illustrated in Figs. 7–8, the marshes are not a net source of particulate COCs to the water column.

The results of the 2014 and 2015 OPTICS monitoring studies conducted in BCSA confirmed several elements of the CSM related to tidal and storm flow movement of dissolved COCs and resuspension and transport of particulate COCs and UPCBs. Fluff layer resuspension and deposition is an important process by which COCs are exchanged from the sediment bed to the water column. The concentrations of TSS, particulate COCs, and UPCBs in UBC and, likely, portions of northern MBC are influenced by resuspension and deposition of unconsolidated particulates from the thin (< 0.5 cm) fluff layer that is present on the surface of the main channel sediment bed. Particulate resuspension from the fluff layer during peak tidal velocities and storm runoff flows resulted in short-term (on the order of hours to days) increases in suspended solids and particulate COC and UPCB concentrations. In turn, particulates and associated COCs deposited to the fluff layer during low velocity periods (e.g., slack tides). Spring tide conditions resulted in higher tidal velocities in the BCSA waterways than neap tides, and a correspondingly greater degree of resuspension of fluff layer particulates from the surface of the waterway sediment bed.

Overall, the temporal patterns in particulate COC, UPCB, and TSS concentrations across the OPTICS monitoring studies were consistent with the BCSA water balance and hydrodynamic and sediment transport models (BCSA Group 2018). These analyses show that influences of storm runoff events are most prominent in UBC, where storm flows can oftentimes be comparable to or greater than tidal flows. OPTICS monitoring data show decreases in TSS and particulate COC and UPCB concentrations, coupled with dampened tidal fluctuations in UBC for an approximate 2-d period following the peak of once-per-year storm events. These results suggest that a large portion of the most mobile fraction of the fluff layer in UBC can be mobilized downstream to MBC and into the marshes as a result of the storm runoff. Although particulate COCs introduced to the water column through fluff layer resuspension move downstream during ebb tides and storm runoff, OPTICS monitoring results and other lines of evidence (e.g., dye studies, field-validated sediment transport modeling; BCSA Group 2018) indicate that the influence of downstream

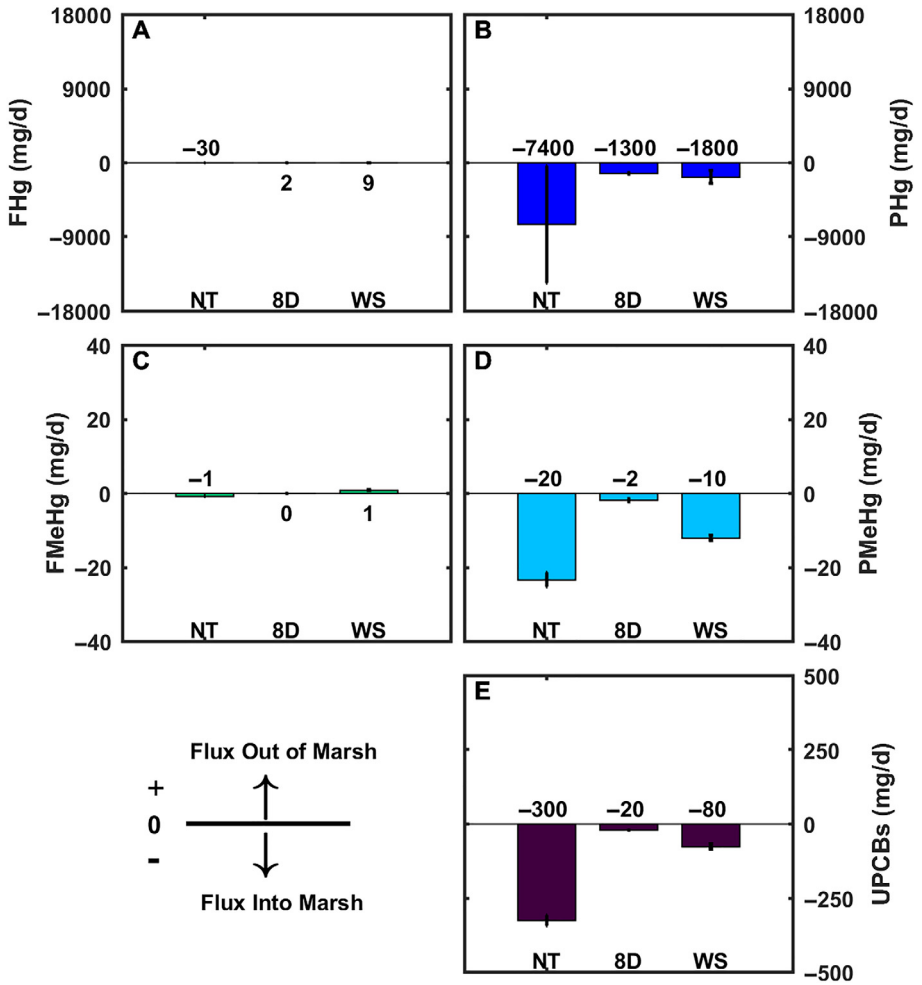


**Fig. 8.** Net daily mass flux averaged over the monitoring period (rounded values provided) for (**A**) FHg, (**B**) PHg, (**C**) FMeHg, (**D**) PMeHg, and (**E**) UPCBs at each marsh tributary monitoring station in 2015. See text for calculations. NT = Nevertouch Marsh, 8D = Eight Day Swamp, and WS = Walden Swamp marsh tributaries.

transport of water column COC concentrations is reduced at the southern end of MBC and in BCC, even during a once-per-year storm event. Infrequent, large magnitude rainfall events (e.g., once every 3–5 yr rainfall magnitudes) are likely necessary to result in appreciable elevation in channel velocities and shear stresses in the southern end of MBC and in BCC.

Further, the marsh tributary mass flux calculations support other lines of evidence suggesting that net transport of TSS, PHg, PMeHg, and UPCBs is from the waterways to the marshes, which is consistent with the net depositional character of the marshes. The marsh tributary monitoring efforts indicated that the transport of FHg and FMeHg out of the marshes as a result of tidal exchange processes is between 1% and 7% of the particulate phase Hg and MeHg mass transported into the marshes during tidal flooding.

In summary, optically based water column monitoring provided high-frequency, robust determinations of water quality conditions and chemical properties, allowing for quantification of chemical contaminant concentrations over

**Table 4.** Net mass flux of COCs (mass flux integrated over the time period of discrete water sampling) estimated from discrete water sample data collected on 30 August 2015 in Nevertouch Marsh and Eight Day Swamp tributaries. Results from OPTICS-derived estimates of net mass flux from Table 3 are in parentheses for comparison. Positive values indicate ebb dominance (out of the marsh) and negative values indicate flood dominance (into the marsh).

| Location | PHg (mg) | PMeHg (mg) | UPCBs (mg) | FHg (mg) | FMeHg (mg) |
|---|---|---|---|---|---|
| Nevertouch Marsh | −9640 (−7431) | −28 (−23) | −763 (−326) | −20 (−30) | −0.9 (−0.7) |
| Eight Day Swamp | −688 (−1301) | −1.7 (−1.9) | −58 (−21) | 6.4 (2.3) | −0.1 (0.1) |

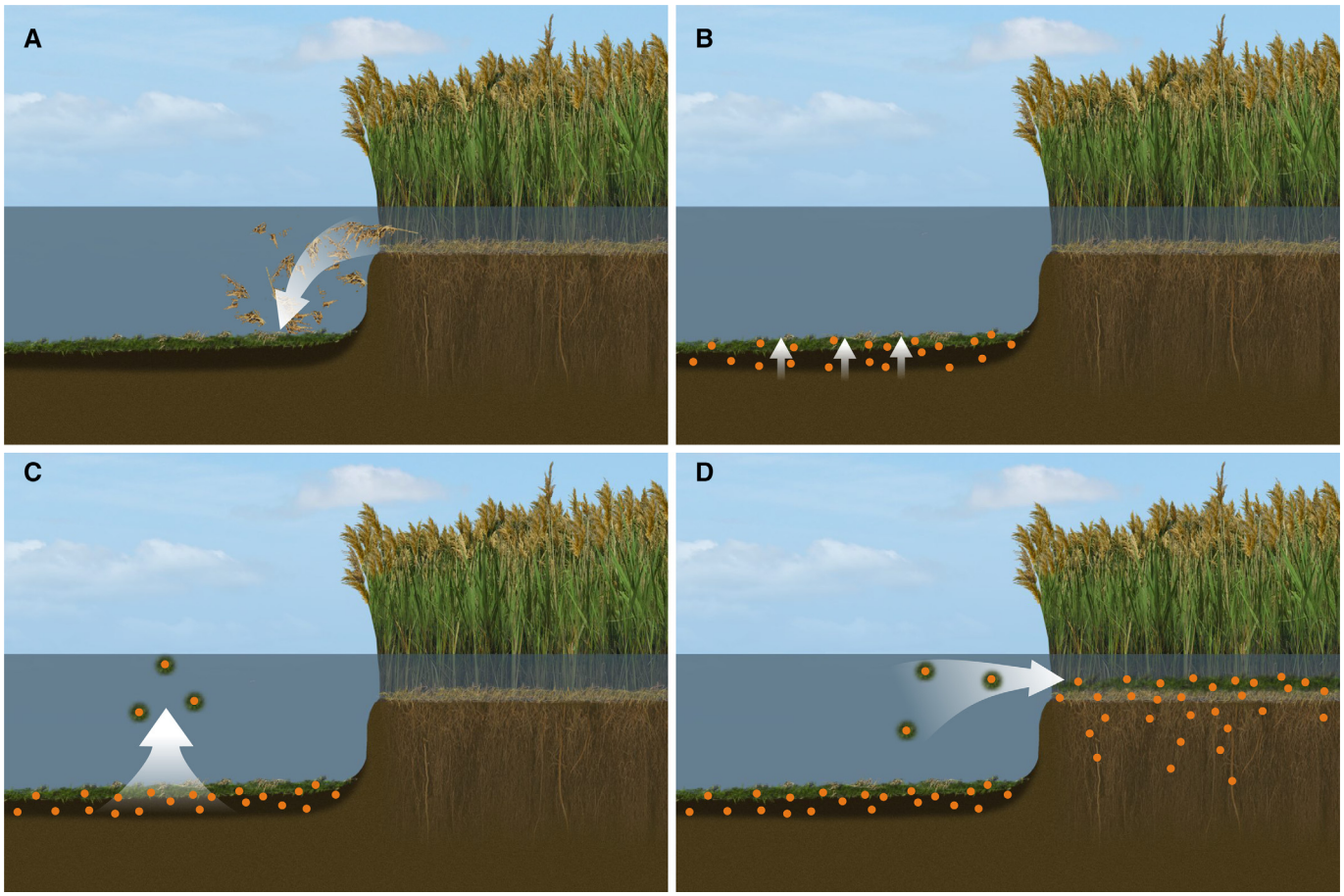


**Fig. 9.** Conceptual site model based on multiple lines of evidence gathered during the BCSA RI program. See text for panel descriptions.

unprecedented temporal and spatial scales. The ability to obtain high frequency chemical data on the order of minutes makes this technique a uniquely powerful and cost-effective tool for monitoring chemical contaminants in the water column. The OPTICS studies provided the link between the roles of waterway sediment, the main channel water column, and marshes on biological exposure routes for mercury, methylmercury, and PCBs, which will help inform remedial actions.

## References

Agrawal, Y. C., and O. A. Mikkelsen. 2009. Empirical forward scattering phase functions from 0.08 to 16 deg. for randomly shaped terrigenous 1-21 micron sediment grains. Opt. Express **17**: 8805–8814. doi:10.1364/OE.17.008805

Babin, M., A. Morel, V. Fournier-Sicre, F. Fell, and D. Stramski. 2003. Light scattering properties of marine particles in coastal and open ocean waters as related to the particle mass concentration. Limnol. Oceanogr. **48**: 843–859. doi: 10.4319/lo.2003.48.2.0843

Bergamaschi, B. A., and others. 2011. Methyl mercury dynamics in a tidal wetland quantified using in situ optical measurements. Limnol. Oceanogr. **56**: 1355–1371, DOI: 10.4319/lo.2011.56.4.1355

Bergamaschi, B. A., and others. 2012*a*. Mercury dynamics in a San Francisco estuary tidal wetland: Assessing dynamics using in situ measurements. Estuaries Coast. **35**: 1036–1048. doi:10.1007/s12237-012-9501-3

Bergamaschi, B. A., D. P. Krabbenhoft, G. R. Aiken, E. Patino, D. G. Rumbold, and W. H. Orem. 2012*b*. Tidally driven export of dissolved organic carbon, total mercury, and methylmercury from a mangrove-dominated estuary. Environ. Sci. Technol. **46**: 1371–1378. doi:10.1021/es2029137

Berry's Creek Study Area Cooperating PRP Group. 2010. Phase 1 site characterization report: Berry's Creek Study Area. U.S. Environmental Protection Agency. New York, NY.

Berry's Creek Study Area Cooperating PRP Group. 2012. Phase 2 site characterization report for remedial investigation/feasibility study: Berry's Creek Study Area. U.S. Environmental Protection Agency. New York, NY.

Berry's Creek Study Area Cooperating PRP Group. 2018. Remedial investigation report, Berry's Creek Study Area remedial investigation. U.S. Environmental Protection Agency. New York, NY.

Boss, E., and W. S. Pegau. 2001. Relationship of light scattering at an angle in the backward direction to the

backscattering coefficient. Appl. Opt. **40**: 5503–5507. doi:10.1364/AO.40.005503

Boss, E., M. S. Twardowski, and S. Herring. 2001*a*. Shape of the particulate beam spectrum and its inversion to obtain the shape of the particle size distribution. Appl. Opt. **40**: 4885–4893. doi:10.1364/AO.40.004885

Boss, E., W. S. Pegau, W. D. Gardner, J. R. V. Zaneveld, A. H. Barnard, M. S. Twardowski, G. C. Chang, and T. D. Dickey. 2001*b*. Spectral particulate attenuation and particle size distribution in the bottom boundary layer of a continental shelf. J. Geophys. Res. **106**: 9509–9516. doi:10.1029/2000JC900077

Briggs, N. T., W. H. Slade, E. Boss, and M. J. Perry. 2013. Method for estimating mean particle size from high-frequency fluctuations in beam attenuation or scattering measurements. Appl. Opt. **52**: 6710–6725. doi:10.1364/AO.52.006710

Chang, G. C., A. H. Barnard, S. McLean, P. J. Egli, C. Moore, J. R. V. Zaneveld, T. D. Dickey, and A. Hanson. 2006. In situ optical variability and relationships in the Santa Barbara Channel: Implications for remote sensing. Appl. Opt. **45**: 3593–3604. doi:10.1364/AO.45.003593

Chen, C. Y., M. Dionne, B. M. Mayes, D. M. Ward, S. Sturup, and B. P. Jackson. 2009. Mercury bioavailability and bioaccumulation in estuarine food webs in the Gulf of Maine. Environ. Sci. Technol. **43**: 1804–1810. doi:10.1021/es8017122

Chen, C. Y., M. E. Borsuk, D. M. Bugge, T. Hollweg, P. H. Balcom, D. M. Ward, J. Williams, and R. P. Mason. 2014. Benthic and pelagic pathways of methylmercury bioaccumulation in estuarine food webs of the Northeast United States. PLoS One **9**: e89305. doi:10.1371/journal.pone.0089305

Coble, P., C. Hu, R. Gould, G. Chang, and M. Wood. 2004. Colored dissolved organic matter in the coastal ocean: An optical tool for coastal zone environmental assessment and management. Oceanogr. Mag. **17**: 50–59. doi:10.5670/oceanog.2004.47

Curran, K. J., P. S. Hill, T. G. Milligan, O. A. Mikkelsen, B. A. Law, X. Durrieu de Madron, and F. Bourrin. 2007. Settling velocity, effective density, and mass composition of suspended sediment in a coastal bottom boundary layer, Gulf of Lions, France. Cont. Shelf Res. **27**: 1408–1421. doi:10.1016/j.csr.2007.01.014

David, N., L. J. McKee, F. J. Black, A. R. Flegal, C. H. Conaway, D. H. Schoellhamer, and N. K. Ganju. 2009. Mercury concentrations and loads in a large river system tributary to San Francisco Bay, California, USA. Environ. Toxicol. Chem. **28**: 2091–2100. doi:10.1897/08-482.1

de Jong, S. 1993. SIMPLS: An alternative approach to partial least squares regression. Chemometr. Intell. Lab. Syst. **18**: 251–263. doi:10.1016/0169-7439(93)85002-X

Di Toro, D. M., and others. 1991. Technical basis for establishing sediment quality criteria for nonionic organic chemicals using equilibrium partitioning. Environ. Toxicol. Chem. **10**: 1541–1583,, DOI: 10.1002/etc.5620101203

Dyer, K. R. 1997. Estuaries: A physical introduction, 2nd ed. Wiley & Sons.

Eggleton, J., and K. V. Thomas. 2004. A review of factors affecting the release and bioavailability of contaminants during sediment disturbance events. Environ. Int. **30**: 973–980. doi:10.1016/j.envint.2004.03.001

Friedrichs, C. T. 2011. Tidal flat morphodynamics: A synthesis, p. 137–170. *In* Edited by J. D. Hansom and B. W. Flemming; Treatise on estuarine and coastal science. Elsevier.

Friedrichs, C. T., and J. E. Perry. 2001. Tidal salt marsh morphodynamics: A synthesis. J. Coast. Res. **27**: 7–37. https://www.jstor.org/stable/25736162

Fugate, D. C., and C. T. Friedrichs. 2003. Controls on suspended aggregate size in partially mixed estuaries. Estuar. Coast. Shelf Sci. **58**: 389–404. doi:10.1016/S0272-7714(03)00107-0

Greenberg, A. E., L. S. Clesceri, and A. D. Eaton [eds.]. 1992. Standard methods for the examination of water and wastewater, 18th ed. American Public Health Association Publications, p. 1100.

Kim, S.-C., C. T. Friedrichs, J. P.-Y. Maa, and L. D. Wright. 2000. Estimating bottom stress in tidal boundary layer from acoustic Doppler velocimeter data. J. Hydraul. Eng. **126**: 399–406. doi:10.1061/(ASCE)0733-9429(2000)126:6(399)

Letz, G. 1983. The toxicology of PCB's—an overview for clinicians. West. J. Med. **138**: 534–540. Obtained from https://www.ncbi.nlm.nih.gov/pmc/articles/PMC1010737/

Lick, W. 2009. Sediment and contaminant transport in surface waters. CRC Press.

Mason, R. P., N. M. Lawson, A. L. Lawrence, J. J. Leaner, J. G. Lee, and G.-R. Sheau. 1999. Mercury in Chesapeake Bay. Mar. Chem. **65**: 77–96. doi:10.1016/S0304-4203(99)00012-2

McCarthy, J. F., and J. M. Zachara. 1998. Subsurface transport of contaminants. Environ. Sci. Technol. **23**: 496–502. doi:10.1021/es00063a001

Mergler, D., H. A. Anderson, L. Hing Man Chan, K. R. Mahaffrey, M. Murray, M. Sakamoto, and A. H. Stern. 2007. Methylmercury exposure and health effects in humans: A worldwide concern. Ambio **36**: 3–11. doi:10.1579/0044-0774(2007)36[3:MEAHEI]2.0.CO;2

Rosipal, R. and N. Krämer. 2006. Overview and recent advances in partial least squares, p. 34–51. *In* Edited by C. Saunders, M. Grobelnik, S. Gunn, and J. Shawe-Taylor, Subspace, latent structure, and feature selection: Statistical and optimization perspectives Workshop (SLSFS 2005), Revised Selected Papers (Lecture Notes in Computer Science), v. 3940. Springer-Verlag.

Scheuhammer, A. M., M. W. Meyer, M. B. Sandheinrich, and M. W. Murray. 2007. Effects of environmental methylmercury on the health of wild birds, mammals, and fish. Ambio **36**: 12–19. doi:10.1579/0044-7447(2007)36[12:EOEMOT]2.0.CO;2

Slade, W. H., and E. Boss. 2015. Spectral attenuation and backscattering as indicators of average particle size. Appl. Opt. **54**: 7264–7277. doi:10.1364/AO.54.007264

Sullivan, J. M., M. S. Twardowski, P. L. Donaghay, and S. A. Freeman. 2005. Use of optical scattering to discriminate particle types in coastal waters. Appl. Opt. **44**: 1667–1680. doi:10.1364/AO.44.001667

Twardowski, M. S., E. Boss, J. B. Macdonald, W. S. Pegau, A. H. Barnard, and J. R. V. Zaneveld. 2001. A model for estimating bulk refractive index from the optical backscattering ratio and the implications for understanding particle composition in case I and case II waters. J. Geophys. Res. **106**: 14129–14142. doi:10.1029/2000JC000404

Ullrich, S. M., T. W. Tanton, and S. A. Abdrashitova. 2001. Mercury in the aquatic environment: A review of factors affecting methylation. Crit. Rev. Environ. Sci. Technol. **31**: 241–293. doi:10.1080/20016491089226

United States Environmental Protection Agency. 2002. Method 1631, Revision E: Mercury in water by oxidation, purge and trap, and cold vapor atomic fluorescence spectrometry. EPA-821-R-02-019. Office of Water, Washington, D.C.

Weis, P., and J. T. F. Ashley. 2007. Contaminants in fish of the Hackensack Meadowlands, New Jersey: Size, sex, and seasonal relationships as related to health risks. Arch. Environ. Contam. Toxicol. **52**: 80–89. doi:10.1007/s00244-006-0093-4

Wright, V. A., and R. P. Blauvelt. 2010. Berry's Creek: A glance backward and a look forward. Int. J. Soil Sediment Water **3**: 1–9. Available at https://scholarworks.umass.edu/intljssw/vol3/iss2/1

Zhang, X., L. Hu, and M.-X. He. 2009. Scattering by pure seawater: Effect of salinity. Opt. Express **17**: 12685–12691. doi:10.1364/OE.17.005698

**Acknowledgments**

Special thanks are extended to Brian Bergamaschi and Bryan Downing for sharing their knowledge and experience with field experiment design, equipment needs, and data analysis. The authors also wish to acknowledge the BCSA Cooperating PRP Group, Judi Durda, Brandon Sackmann, and The ELM Group (Peter Brussock and Jennifer Wollenberg) for project support; Michael Twardowski for field equipment; and Ian Stupakoff and Nicholas Shonka, and Geosyntec Consultants (Nicholas Muenks, Russel Hyatt, Jared Brisman, Cody Luebbering, Jedidiah Sirk, Courtney Thomas, and many others) for field support.

**Conflict of Interest**

None declared.

*Submitted 18 December 2017*
*Revised 1 June 2018*
*Accepted 12 July 2018*

*Associate editor: Luiz Drude de Lacerda*